

pelvis and head and neck, in lung instead, gamma pass rates were lower in 4/5 cases.

**Conclusion:** DC is a suitable tool for VMAT in vivo dosimetry. The pencil beam algorithm can be inaccurate in the presence of low-density inhomogeneities.

#### PO-0826

**Benchmarking computed IDD curves for four proton treatment planning systems against measured data**

J. Alshaiqi<sup>1,2</sup>, D. D'Souza<sup>2</sup>, C.G. Ainsley<sup>3</sup>, I. Rosenberg<sup>2</sup>, G. Royle<sup>1</sup>, R.A. Amos<sup>2</sup>

<sup>1</sup>University College London, Medical Physics & Biomedical Engineering, London, United Kingdom

<sup>2</sup>University College London Hospitals, Radiotherapy Physics, London, United Kingdom

<sup>3</sup>University of Pennsylvania, Roberts Proton Therapy Center, Philadelphia, USA

**Purpose or Objective:** Accurate beam modelling is an essential function of a treatment planning system (TPS) to ensure that plans can be calculated that are deliverable within clinically acceptable tolerances. The purpose of this work is to evaluate the computed integral depth dose (IDD) curves of four commercially available proton TPSs, benchmarked against measured data. The four TPSs (EclipseTM, XiO®, Pinnacle3, RayStation®) were commissioned using pencil beam scanning data from the University of Pennsylvania (UPenn) facility.

**Material and Methods:** A water cube phantom (40cm<sup>3</sup>) was created in each TPS for calculation of IDD curves. Calculation grid size set to 1mm in all TPSs. Individual IDDs for 27 nominal energies, ranging from 100 to 226.7MeV, were calculated by integrating the calculated depth dose distributions. These were all benchmarked against measured data from UPenn, comparing the clinical range at 80% distal dose (D80), Bragg peak width between distal and proximal 80% (D80-P80), range at 0.5% (R0.5), and distal penumbra between D80 and R0.5. Gamma-index analysis with pass criteria of 1mm/1% was also used to compare computed and measured IDDs.

**Results:** Mean percentage of IDDs with >95% pass rate for 1mm/1% criteria were 96.7% (SD 4.9) for XiO®, 94.1% (SD 8.9) for EclipseTM, 95.4% (SD 8.6) for RayStation®, and 49.2 (SD 26.0) for Pinnacle3. Maximum differences between computed and measured IDD data are shown below. No correlation with nominal energy was observed.

	Maximum differences [mm]			
	Range 80% (D80)	Peak width (D80-P80)	Distal penumbra (D80-R0.5)	Range 0.5% (R0.5)
XiO®	0.1	0.1	0.2	0.2
Eclipse™	0.8	0.6	1.1	1.2
RayStation®	0.3	0.4	0.8	0.8
Pinnacle <sup>3</sup>	0.4	0.6	0.9	1.3

**Conclusion:** Characteristics of computed IDDs were compared to measured data for four commercially available TPSs. All were within clinically acceptable tolerances, with XiO showing the closest agreement. Differences observed were attributed to TPS specific beam modelling. Further investigation will assess the cumulative impact of these discrepancies on verified clinical treatment plans.

#### PO-0827

**Principal component analysis for deviation detection in 3D in vivo EPID dosimetry**

R.A. Rozendaal<sup>1</sup>, B. Mijnheer<sup>1</sup>, I. Olaciregui-Ruiz<sup>1</sup>, P. Gonzalez<sup>1</sup>, J.J. Sonke<sup>1</sup>, A. Mans<sup>1</sup>

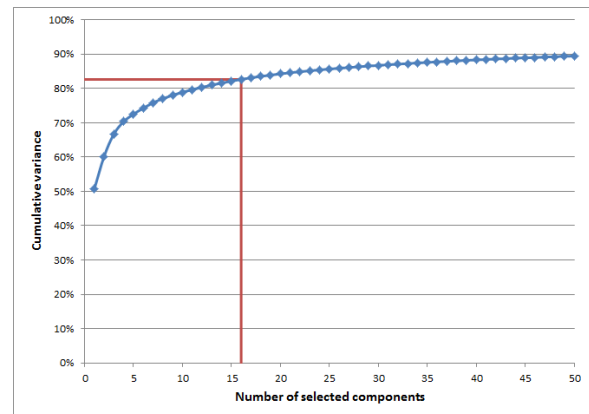
<sup>1</sup>Netherlands Cancer Institute Antoni van Leeuwenhoek Hospital, Department of Radiotherapy Physics, Amsterdam, The Netherlands

**Purpose or Objective:** One of the clinical issues our institute faces regarding in vivo EPID dosimetry is the number of raised alerts. For example, alerts are raised for 49% of the treatments in case of head-and-neck (H&N) VMAT treatments; an alert is raised when dosimetry results are

found deviating according to statistics derived from the histogram of 3D  $\gamma$ -analysis results. These alerts are mostly found to be patient-related or attributable to limitations of our back-projection and dose calculation algorithm. After inspection, an intervention is considered for only 0.3% of the treatments. The purpose of this study is to develop a principal component analysis (PCA) based classification method to improve the specificity of our EPID dosimetry system. In particular, in contrast to our current classification method, PCA allows for the spatial distribution of  $\gamma$ -values to be taken into account for deviation detection.

**Material and Methods:** The input for PCA consisted of 3D  $\gamma$ -distributions (3%/3mm), one per treatment arc per fraction. In total, 2024 3D  $\gamma$ -distributions from 499 H&N VMAT treatment-plans were included. As an initial choice, components describing at least 1% of the variance were selected. The distribution of variances over the components was inspected to validate this choice. Using these components, new 3D  $\gamma$ -distributions were created by projecting each input 3D  $\gamma$ -distribution on only these components and then projecting the result to the original coordinate system of the 3D  $\gamma$ -distributions. If the selected components describe the original  $\gamma$ -distribution well, the new and original  $\gamma$ -distributions will be similar. This similarity was quantified by the root mean square (RMS) d of the difference between the two  $\gamma$ -distributions; a  $\gamma$ -distribution was marked as deviating when d exceeded a threshold. All true positive  $\gamma$ -distributions (n = 2) in the dataset, as identified by experienced medical physicists, were used to determine this threshold for identification of alerts.

**Results:** The first 16 components were each found to describe at least 1% of the variance; cumulatively, they account for 83% of the variance in the dataset. Figure 1 shows the cumulative variance accounted for as a function of selected components and indicates that the choice for selecting components is reasonable. After finding and applying the appropriate threshold for detecting the identified true positives, a drop in alert rate from 49% to 11% was observed, corresponding to an increase in specificity from 0.51 to 0.89.



**Conclusion:** The PCA-based classification method presented in this study enhances the specificity of deviation detection in 3D in vivo EPID dosimetry of H&N VMAT from 0.51 to 0.89, compared to our current clinical  $\gamma$ -histogram based method. Before clinical implementation, a rigorous validation is required.

#### PO-0828

**Dosimetric assessment of a second generation Multi-Leaf Collimator for robotic radiotherapy**

P.H. Mackeprang<sup>1</sup>, D. Schmidhalter<sup>1</sup>, D. Henzen<sup>1</sup>, M. Malthaner<sup>1</sup>, D.M. Aebbersold<sup>1</sup>, P. Manser<sup>1</sup>, M.K. Fix<sup>1</sup>

<sup>1</sup>Division of Medical Radiation Physics and Department of Radiation Oncology Inselspital, Bern University Hospital, and University of Bern, Switzerland

**Purpose or Objective:** Recently, a second generation Multi-Leaf Collimator (InCise 2™) was released for the CyberKnife® M6™ robotic radiotherapy system. As part of the evaluation and initial characterization, physical, dosimetric and planning parameters were recorded. Further, planning studies on phantoms were performed to compare the InCise 2 to the Iris™ collimator system.

**Material and Methods:** As part of the InCise 2 validation, leakage, TG-50 picket fence, Bayouth fence and automated quality assurance measurements were performed using radiochromic film. End to end delivery tests were performed for skull-, fiducial-, x-sight spine-, x-sight lung- and synchrony tracking. Ten treatment plans and five QA plans were delivered to phantoms using the InCise 2. Ionization chamber measurements as well as film measurements were compared with dose calculated by the treatment planning system. For dosimetric assessment, treatment plans to water phantoms were generated using the IRIS collimator system and the InCise 2 MLC. On a cylindrical water phantom of a diameter of 20 cm, spherical target volumes of diameters from 5 to 80 mm were drawn. Firstly, the dose optimization algorithm using the MLC was assessed using a simple Optimize Minimum Dose (OMI) objective. Secondly, shell volumes were generated around the target volumes and their coverage was optimized (OCI). 1000 cGy were prescribed to the 80% isodose. Dose distributions, Nakamura's new Conformity Index (nCI) as well as optimization and estimated treatment times were analyzed.

**Results:** All validation tests were passed within tolerances. Maximum leakage was recorded as 0.44% for all MLC orientations. Mean leaf positioning errors in Bayouth fence tests ranged from -0.043 mm to 0.006 mm, without any individual leaves exceeding the tolerance of  $\pm 0.27$  mm. All phantom plans were delivered successfully, with recorded dose for QA plans differing 1.94%  $\pm 1.03\%$  from calculated dose and gamma analysis (3% / 1mm, 20% dose threshold) showing > 97% agreement. Total end to end tracking errors were below 0.95 mm for all tested tracking methods. Testing the optimization algorithm revealed nCI values for plans optimized based on target volume shells between 1.02 and 1.50 for plans using the InCise 2 and 1.05 and 1.43 for IRIS. MLC optimization times increased as a function of both target size and optimization steps, ranging from 12 s for the 5 mm PTV OMI plan to 7 h for the 80 mm PTV shell based optimization. Estimated treatment times including setup times for the synthetic plans were reduced by a mean of 19.1% when choosing the InCise 2 over the IRIS.

**Conclusion:** The InCise 2 MLC system passed initial physics evaluation at our site and showed dose distributions comparable to the CyberKnife IRIS collimator system for spherical targets. Estimated MLC treatment times are about 20% lower compared to the IRIS collimator system.

#### PO-0829

Determining the mechanical properties of a radiochromic deformable silicone-based 3D dosimeter

L.P. Kaplan<sup>1</sup>, E.M. Høye<sup>2</sup>, P. Balling<sup>1</sup>, L.P. Muren<sup>2</sup>, J.B.B. Petersen<sup>2</sup>, P.R. Poulsen<sup>2</sup>, E.S. Yates<sup>2</sup>, P.S. Skyt<sup>2</sup>

<sup>1</sup>Aarhus University, Dept. of Physics and Astronomy, Aarhus C, Denmark

<sup>2</sup>Aarhus University/Aarhus University Hospital, Dept. of Oncology, Aarhus C, Denmark

**Purpose or Objective:** Recently emerged radiotherapy methods such as intensity-modulated or image-guided radiotherapy are capable of delivering very conformal dose distributions to patients, but their accuracy can be greatly compromised by e.g. the deformation of organs in the patient. The accuracy of deformable registration algorithms developed to correct for this is not well known due to the challenging nature of deformation measurements. A new type of deformable radiochromic 3D dosimeter consisting of a silicone matrix has recently been developed in our group. This dosimeter makes direct dose measurements in deformed geometries possible. The aim of this study was to investigate

its mechanical properties in terms of tensile stress and compression.

**Material and Methods:** The dosimeter contained the SYLGARD® 184 Silicone Elastomer kit (Dow Corning), Leuco-Malachite Green (LMG) dye as the active component and chloroform as solvent and sensitizer. To determine the shape of the dosimeter's stress-strain curve and Young's modulus (Y), tensile stress was imposed on rod shaped samples along their central axis and the resulting strain was observed using a camera. To define Y a linear approximation was made for small strains. This was done at varying times after production, for varying curing agent concentrations and for both irradiated and non-irradiated dosimeters.  $10 \times 10$  cm<sup>2</sup> photon fields with beam quality 6 MV were used to deliver a dose of 60 Gy at 600 MU/min. To investigate whether the density of the material is conserved under compression, dosimeters were CT-scanned while placed in a wooden clamp to impose varying degrees of compressive stress. Finally, dosimeters were also partially irradiated while subject to tensile stress to see if the irradiated areas would return to the original geometry once the stress was removed after irradiation.

**Results:** The measured stress-strain curves did not show hysteresis or plastic deformation, even after multiple deformations. Y was found to be 0.08-0.2 MPa 48 hours after production depending on the amount of curing agent (see figure), and it increased at an exponentially decreasing rate for up to several weeks afterwards due to further hardening. Irradiation prior to imposing tensile stress did not affect the mechanical properties immediately, but it slowed the hardening process in the following days. The volume was found to be conserved during compressive stress of up to 60%. Multiple tests showed that dosimeters irradiated partially under tensile stress returned completely to their original geometries after removing the stress (see table).

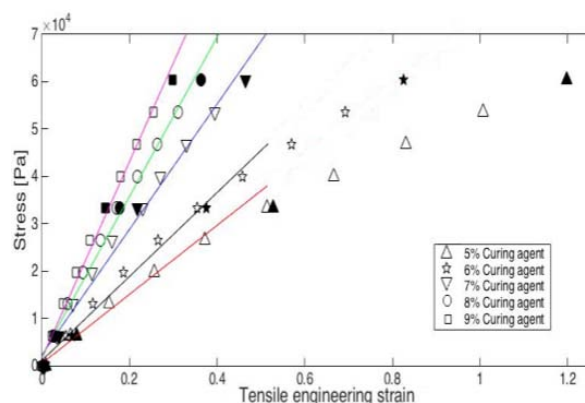


Figure 1: Stress-strain curve for dosimeters with varying curing agent concentrations 48 hours after production. The un-filled markers indicate measurements taken while loading, while the filled markers show measurements taken while unloading. Notice that these coincide well with the un-filled markers, indicating the absence of hysteresis. Linear fits are included for strains smaller than 0.5. Error bars are not included, as they are smaller than the markers.

Table 1.1: Dosimeters irradiated under tensile strain. All dosimeters were irradiated with a field 0.5 cm wide.

Original length of irradiated area (no strain) <sup>1</sup> (cm)	Length after irradiation(cm)
0.5	0.5
0.44	0.48
0.41	0.41
0.38	0.39
0.34	0.34
0.31	0.32
0.28	0.28
0.25	0.27
0.19	0.21

<sup>1</sup> Due to the setup there was an uncertainty of  $\approx \pm 0.05$  cm in determining the original length of the areas to be irradiated.